The cuproptosis-related gene signature serves as a potential prognostic predictor for ovarian cancer using bioinformatics analysis

Xin Sun[1]^, Panling Xu[1]^, Fengli Zhang[1]^, Ting Sun[1]^, Haili Jiang[1]^, Xinyuan Lu[2]^, Mei Zhang[1]^, Ping Li[1]^

[1]Department of Traditional Chinese and Western Oncology, The First Affiliated Hospital of Anhui Medical University, Hefei, China; [2]The Graduate School, Anhui University of Traditional Chinese Medicine, Hefei, China

Contributions: (I) Conception and design: X Sun, P Li; (II) Administrative support: X Sun, P Li; (III) Provision of study materials or patients: X Sun, P Xu, F Zhang; (IV) Collection and assembly of data: X Sun, T Sun, H Jiang, X Lu; (V) Data analysis and interpretation: X Sun, P Li, P Xu, M Zhang; (VI) Manuscript writing: All authors; (VII) Final approval of manuscript: All authors.

Correspondence to: Ping Li. Department of Traditional Chinese and Western Oncology, The First Affiliated Hospital of Anhui Medical University, Anhui 230022, China. Email: 1964liping@sina.com.

Background: Studies have shown that copper is involved in the tumorigenesis and development of ovarian cancer. In this work, we aimed to build a prognostic classification system associated with cuproptosis to predict ovarian cancer prognosis.

Methods: Information of ovarian cancer samples were acquired from The Cancer Genome Atlas (TCGA)-ovarian cancer and GSE26193 dataset. Cuproptosis-related genes were screened from previous research. ConsensusClusterPlus was applied to determine molecular subtypes, which were evaluated by tumor immune microenvironment analysis, TIDE algorithm, and functional enrichment analysis. Furthermore, limma analysis and univariate Cox analysis were used to construct a cuproptosis-related prognostic signature for ovarian cancer. Univariate and multivariate Cox regression analyses were used to analyze the independence of clinical factors and model.

Results: A total of 15 genes related to cuproptosis were identified, and 2 clusters (C1 and C2) were determined. C1 had a better survival outcome, less advanced stage, enhanced immune infiltration, was more sensitive to immunotherapy, and showed enrichment in tricarboxylic acid (TCA)-related pathways. An 8 cuproptosis-associated gene signature was constructed, and the signature was verified in the GSE26193 dataset. A higher risk score of the cuproptosis-related gene signature was significantly correlated with worse overall survival (OS) ($P<0.0001$), which was validated in GSE26193 dataset successfully. Cox survival analysis showed that risk score was an independent predictor [hazard ratio (HR) =2.66, $P<0.001$]. Functional enrichment and tumor immune microenvironment analyses showed that high-risk patients tended to have immunologically sensitive tumors.

Conclusions: The cuproptosis-related gene signature may serve as a potential prognostic predictor for ovarian cancer patients and may offer novel treatment strategies for ovarian cancer.

Keywords: Ovarian cancer; cuproptosis; clusters; signature; prognosis

Submitted Sep 08, 2022. Accepted for publication Sep 22, 2022.
doi: 10.21037/atm-22-4546
View this article at: https://dx.doi.org/10.21037/atm-22-4546

^ ORCID: Xin Sun, 0000-0002-1093-6801; Panling Xu, 0000-0003-1592-5527; Fengli Zhang, 0000-0002-7006-4312; Ting Sun, 0000-0002-5994-3228; Haili Jiang, 0000-0003-4392-7642; Xinyuan Lu, 0000-0001-7655-7970; Mei Zhang, 0000-0001-6221-6315; Ping Li, 0000-0003-0958-6784.

Introduction

Ovarian cancer is one of the most common cancers in women, with a high incidence rate. Among gynecological malignant tumors, ovarian cancer has a very poor prognosis and the lowest survival rate. Statistics showed that in 2020 alone, nearly 320,000 women were diagnosed with ovarian cancer worldwide, resulting in nearly 210,000 deaths each year, making it the cancer with the highest mortality rate among gynecological tumors (1). In China, the annual incidence of ovarian cancer ranks third in female reproductive system tumors, and shows an increasing trend year by year. Ovarian cancer is the most frequently diagnosed malignant tumor of the female reproductive system, which seriously threatens women's health and causes a great economic burden to society (2). Studies have shown that the stage of ovarian cancer affects the prognosis of patients. The prognosis of patients with early ovarian cancer is significantly better than patients with advanced ovarian cancer, and early identification of ovarian cancer can improve survival by 10–30% (3,4). In current clinical practice, serum carbohydrate antigen 125 (CA125), human Epididymis protein 4 [human epididymis protein), HE4] and other traditional tumor markers are of great significance in assisting the diagnosis of ovarian cancer and judging the therapeutic effect of tumor. However, there are still problems of poor prognosis and high recurrence rate in ovarian cancer patients. The main reason for this situation may be that people have not fully grasped the pathological molecular mechanism of ovarian cancer, and lack of specific biomarkers as molecular targets for the diagnosis and treatment of ovarian cancer. Therefore, screening and early diagnosis are of great significance to the prognosis of ovarian cancer patients.

Overload or deficiency of copper can lead to impaired cell function and ultimately cell death (5). Tsvetkov *et al.* (6) proposed a novel form of cell death in March 2022, named "cuprotosis", different from the already known regulated cell death processes. This form of cell death depends on copper and can be regulated, and is closely related to mitochondrial respiration. Cuprotosis occurs through direct binding of copper to the lipoacylated component of the tricarboxylic acid (TCA) cycle through lipoacylated protein aggregation and subsequent loss of Fe-S cluster proteins, leading to protein toxic stress and eventual cuprotosis (6). Studies have shown that the content of copper ions in the serum and solid tumor tissues of cancer patients is significantly higher than that of healthy subjects (7,8), and the increase of copper ions can promote the proliferation and metastasis of tumor cells and promote angiogenesis (9). Ren *et al.* found that disulfiram (DSF)/copper could damage mitochondrial homeostasis in hepatocellular cancer (HCC) cells, resulting in mitochondrial fragmentation and aggregation around the nucleus (10). Yang *et al.* showed that the increase of intracellular copper contributes to the radioresistance of HCC cell lines (11). Cuproptosis-related gene signature to predict prognosis have been reported in hepatocellular carcinoma (12), Clear Cell Renal Cell Carcinoma (13), cervical cancer(14).

In this research, we intended to comprehensively investigate the molecular alterations and clinical relevance of cuproptosis-related genes in ovarian cancer. Our analysis highlights the importance of cuproptosis-related genes in ovarian cancer development and lays a foundation for the therapeutic application of cuproptosis regulators for ovarian cancer. We present the following article in accordance with the TRIPOD reporting checklist (available at https://atm.amegroups.com/article/view/10.21037/atm-22-4546/rc).

Methods

This study provides new ideas for the prognosis of ovarian cancer through the construction of molecular subtypes, the screening of key genes and the establishment of a prognostic model.

Raw data

RNA-seq data, clinical information, and copy number variation (CNV) data were acquired from The Cancer Genome Atlas (TCGA)-ovarian cancer and GSE26193 dataset. Samples with clinical information, survival time, and status were retained. Finally, 368 and 107 ovarian cancer samples were included in TCGA-ovarian cancer and GSE26193 dataset, respectively (*Table 1*). The study was conducted in accordance with the Declaration of Helsinki (as revised in 2013). Cuprotosis-related genes were obtained from previous research (6). Scores of cuprotosis-related genes in each sample were calculated by single-sample gene set enrichment analysis (ssGSEA). Subsequently, correlations between all genes and scores were analyzed by Pearson correlation analysis using the selection criteria $|R|>0.3$ and P value <0.001 to obtain genes associated with cuproptosis.

Table 1 Clinical features of samples in TCGA and GSE26193 dataset

Clinical features	TCGA-OV	GSE26193
OS		
Alive	129	27
Dead	239	80
Age (years)		
≤60	199	–
>60	169	–
Stage		
I	1	–
II	21	–
III	287	–
IV	56	–
Unknown	3	–
Grade		
G1	1	–
G2	42	–
G3	315	–
G4	1	–
Unknown	9	–

TCGA-OV, The Cancer Genome Atlas-ovarian cancer; OS, overall survival.

Cluster analysis

As per the standard of P<0.05, cuprotosis-related genes associated with the prognosis of ovarian cancer were obtained via univariate Cox survival analysis using the coxph function of survival package. Molecular subtypes were determined separately for TCGA-CESC dataset samples via ConsensusClusterPlus 1.52.0 (15). Subsequently, "hc" arithmetic and "Pearson" distance were utilized to complete 500 bootstraps with every bootstrap having specimens (≥80%) of TCGA-ovarian cancer dataset. The cluster number k was between 2 and 10, and the optimum k was identified as per the cumulative distribution function (CDF) and area under the curve (AUC). Survival curves [Kaplan-Meier (KM) curves] between molecular subtypes were then analyzed for differences. In addition, differences in the distribution of clinical characteristics between molecular subtypes were compared and a chi-square test was completed, with P<0.05 indicating statistical significance.

Microenvironment cell populations-counter (MCP-counter)

The abundance of immune-infiltrating cells, 8 immune populations [T cells, CD8+ T cells, cytotoxic lymphocytes, natural killer (NK) cells, B cell lineages, monocytic lineages, myeloid dendritic cells, and neutrophils], and 2 stromal cell populations (endothelial cells and fibroblasts) in each sample was assessed with the MCP-counter (16).

ssGSEA

To evaluate the various pathway scores (17), ssGSEA was performed using the R package gene set variation analysis (GSVA).

ESTIMATE algorithm

R software ESTIMATE arithmetic (18) was utilized to compute the overall stroma level (stromal score), immunocyte infiltration (immune score), and ESTIMATE score in TCGA-ovarian cancer cohort using Wilcoxon test analysis to determine differences.

Immunotherapy

The expression levels of 47 immune checkpoint genes, which were obtained from HisgAtlas (19), were determined.

Construction of a prognostic model for ovarian cancer

Differentially expressed genes between clusters were determined using the R limma package with false discovery rate (FDR) <0.05 and $|\log FC| > \log_2(1.5)$.

As per the standard of P<0.01, differentially expressed genes associated with the prognosis of ovarian cancer were determined via univariate Cox survival analysis using the coxph function of survival package.

KM survival curves and receiver operating characteristic (ROC) curves (AUC >0.6) were used to evaluate the ability of the model to predict the prognosis of ovarian cancer.

Independent prognostic power of the risk score

Univariate and multivariate Cox regression analyses were used to examine the independent prognostic power of the

risk score, and Sangerbox was used for analysis (20).

Statistical analysis

R (https://www.r-project.org/, version 3.6.3) helped in all statistical analysis and data visualization. All estimated P values were double-tailed, with a significance level of $P<0.05$.

Results

Identification and mutation analysis of genes associated with cuproptosis

Based on ssGSEA and Pearson analysis, 787 genes associated with cuproptosis were obtained. Then, univariate Cox survival analysis identified 15 genes (*MGST3*, *PDLIM7*, *HIVEP1*, *MPC1*, *KBTBD3*, *SDHD*, *KMT2D*, *ZFHX2*, *MMP25*, *COX4I1*, *ATP2A3*, *TUBB6*, *HDGFL2*, *FXYD5*, *CHKB*) associated with the prognosis of ovarian cancer patients.

A total of 40 (9.17%) of the 436 samples in TCGA-ovarian cancer dataset were mutated (*Figure 1A*). Next, we found that 15 genes had higher copy number amplifications or deletions (*Figure 1B*). Based on CNVs, TCGA-ovarian cancer samples were divided into 3 groups, namely amplification, deletion, and diploid. Compared with deletion, samples in the amplification and diploid groups presented higher gene expression (*Figure 1C*).

Identification of clusters based on 15 genes associated with cuproptosis

Based on 15 genes, ConsensusClusterPlus analysis indicated that when k=2, 2 clusters, namely C1 and C2, were determined in TCGA-ovarian cancer dataset (*Figure 2A-2C*). KM survival analysis showed that patients in C1 had a long survival outcome in TCGA-ovarian cancer dataset (*Figure 2D*). A similar phenomenon was observed in the GSE26193 dataset (*Figure 2E*). Clinical feature distribution of the 2 clusters indicated that stage and status had significance (*Figure 3*).

Analysis of the tumor immune microenvironment

We speculated that subtypes may reflect different immune enrichment. Firstly, ESTIMATE analysis showed that C1 patients had higher stromal scores and ESTIMATE scores (*Figure 4A*). Subsequently, we evaluated the scores of 10 kinds of immune cells using MCP-counter methods, and most cells were highly enriched in C1 (*Figure 4B*). Immune checkpoint inhibitor (ICI) therapy represented by anti-PD-1/L1 agents have undoubtedly made a great breakthrough in anti-tumor therapy. Therefore, 47 immune checkpoint genes were acquired from the HisgAtlas database, and 38 immune checkpoint genes had obviously high expression in C1 compared with C2 (*Figure 4C*).

There were significant differences in B cells and macrophages between the 2 molecular subtypes (*Figure 4B*). Macrophages play an important role in immune regulation. Thus, the scores of the Toll-like receptor signaling pathway, NK cell-mediated cytotoxicity, antigen processing and presentation, and the B cell receptor signaling pathway were calculated using ssGSEA, and Toll-like receptor score, NK cell cytotoxicity score, and B cell receptor signaling pathway score were higher in C1 compared with C2 (*Figure 4D-4G*). The cytolytic activity (CYT) score was also higher in C1 (*Figure 4H*).

Functional enrichment analysis of clusters

GSEA showed that cancer-related pathways, such as pathways in cancer, bladder cancer, and the Wnt signaling pathway, were activated in C1 (*Figure 5A*). Research has indicated that cuproptosis is closely related to the TCA. Thus, we calculated TCA-related pathway scores using ssGSEA methods, and analysis showed that most pathways had significant differences between the 2 clusters (*Figure 5B*). Scores of pathways related to cell growth and death showed that cellular senescence and the p53 signaling pathway had obvious differences between the 2 clusters (*Figure 5C*).

Identification of hub genes associated with cuproptosis

Using limma analysis, 2,058 differentially expressed genes were determined (*Figure 6A*). Next, univariate Cox survival analysis screened 8 genes, all of which were downregulated in C1 (*Figure 6B,6C*). Finally, the formula of the prognostic model was as follows:

$$\begin{aligned} Risk\ score = {} & 0.015\times AMER1 - 0.009\times ATP2A3 - 0.066\times HIPK2 - \\ & 0.137\times RRP12 - 0.042\times VANGL1 - 0.108\times JAG2 - \\ & 0.114\times GALNT6 - 0.115\times CD79A \end{aligned} \quad [1]$$

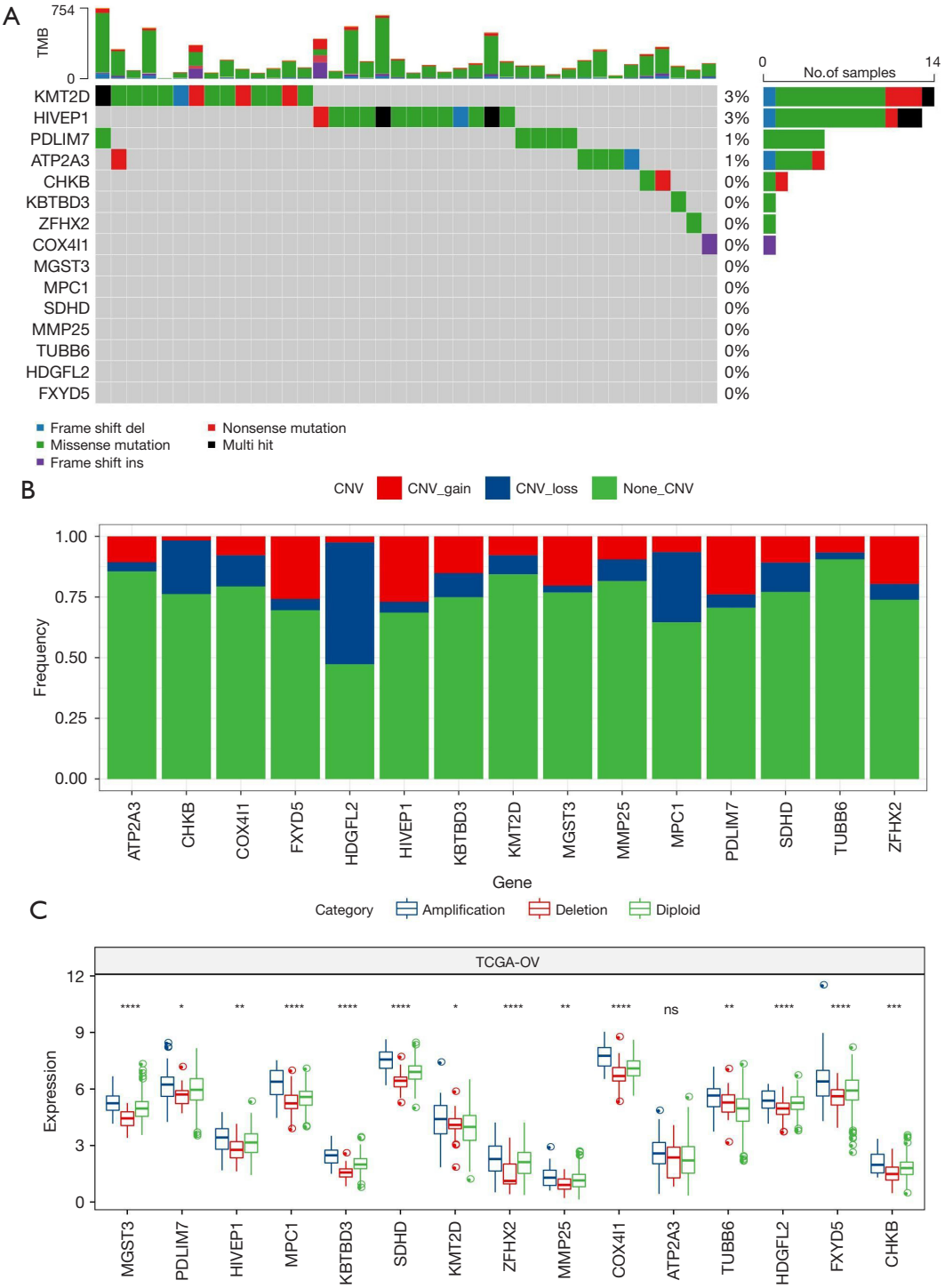

Figure 1 Mutation analysis of genes associated with cuproptosis. (A) Mutation frequency of genes in TCGA-ovarian cancer samples. (B) Copy number variations of genes. (C) Gene expression in the amplification group, deletion group, and diploid group. *P<0.05; **P<0.01; ***P<0.001; ****P<0.0001. TMB, tumor mutation burden; CNV, copy number variation; TCGA, The Cancer Genome Atlas; ns, no significance.

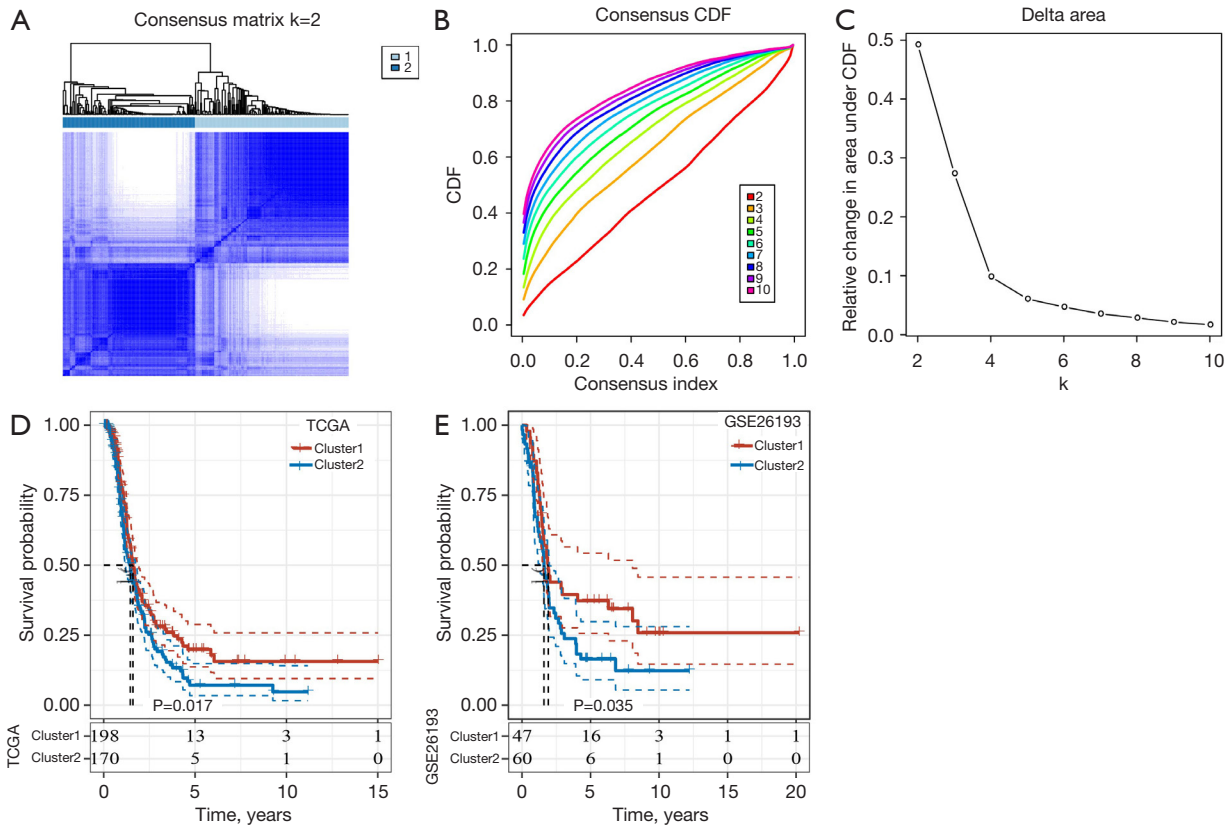

Figure 2 Identification of clusters. (A) Heatmap of clustering when k=2. (B) Cumulative distribution function curve. (C) Cumulative distribution function delta area. (D) KM survival curve between cluster 1 and cluster 2 in TCGA-ovarian cancer dataset. (E) KM survival curve between cluster 1 and cluster 2 in the GSE26193 dataset. CDF, cumulative distribution function; TCGA, The Cancer Genome Atlas; KM, Kaplan-Meier.

Validation of the risk score

Next, the risk score of patients in TCGA-ovarian cancer dataset was calculated according to the above formula. Then, patients were divided into the high group and low group. The AUCs for 1-, 2-, 3-, and 4-year survival in the TCGA-ovarian cancer cohort were 0.61, 0.64, 0.64, and 0.73, respectively (*Figure 7A*). The KM survival curve showed that the low group had good performance in terms of overall survival (OS) compared with the high group in TCGA-ovarian cancer dataset (*Figure 7B*). In the GSE26193 cohort, the AUCs for 1-, 2-, 3-, 4-, and 5-year survival were 0.63, 0.64, 0.69, 0.7, and 0.71, respectively (*Figure 7C*), and samples in the low group had a better survival time compared with the high group (*Figure 7D*). In terms of the distributional status of the 2 groups, there was marked diversity in stage and status (*Figure 8*). Univariate and multivariate Cox survival analysis indicated that risk score was an independent prognostic factor (*Figure 9A,9B*).

Analysis of the tumor immune microenvironment between the 2 groups

ESTIMATE analysis showed that the low group had higher stromal scores, immune scores, and ESTIMATE scores (*Figure 10A*). MCP-counter method results showed that 10 kinds of immune cells were highly enriched in the low group (*Figure 10B*). A total of 42 of 47 immune checkpoint genes had obviously high expression in the low group compared with the high group (*Figure 10C*). The scores of 20 of the 28 kinds of immune cells were higher in the low group compared with those in the high group, as calculated by ssGSEA (*Figure 10D*). The scores of the Toll-like

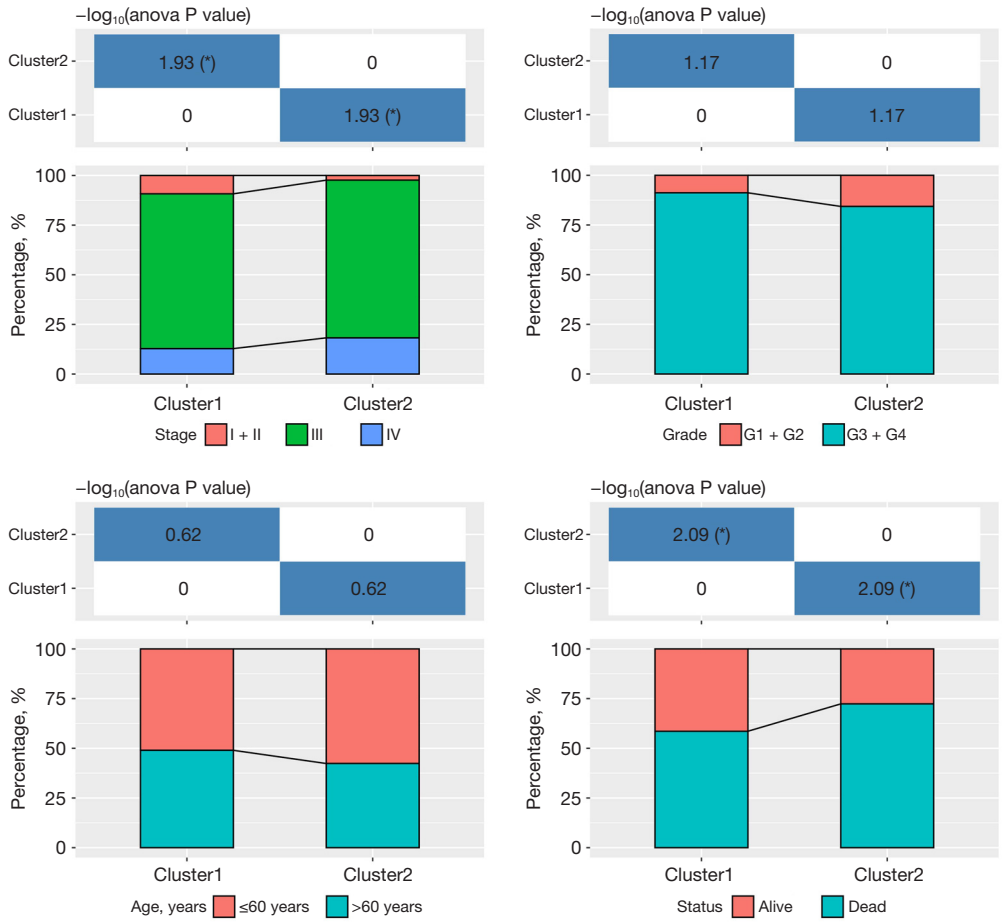

Figure 3 The distributions of clinical features, stage, grade, age, and status in the 2 clusters. *P<0.05.

receptor signaling pathway, NK cell mediated cytotoxicity, and antigen processing and presentation were all higher in the low group compared with those in the high group (*Figure 10E-10G*). The CYT score was also higher in the low group (*Figure 10H*).

TCA pathway analysis of risk score

Most TCA-related pathway scores were significantly different between the 2 groups, and the high group had higher TCA pathway scores (*Figure 11A*). Heatmap analysis indicated that the high group had higher TCA pathway scores (*Figure 11B*). The average of the TCA pathway scores was used as the TCA score, and correlation analysis showed that TCA score was positively correlated with risk score (P=0.0066, *Figure 11C*).

Discussion

To the best of our knowledge, there have been no previous studies exploring the correlation between cuproptosis and the prognosis of ovarian cancer. Surprisingly, based on cuproptosis subtype-related genes, we determined 2 clusters, which had obvious differences in prognosis, immune infiltration, immunotherapy, and TCA pathways. In addition, a novel 8 cuproptosis-related gene prognostic score for ovarian cancer was constructed for the first time, which had good prognostic ability and was an independent prognostic factor. These data indicated the potential role of cuproptosis in the prognosis of ovarian cancer and the predictive value of this score in the prediction of ovarian cancer survivorship.

Studies have shown that copper ions are involved in

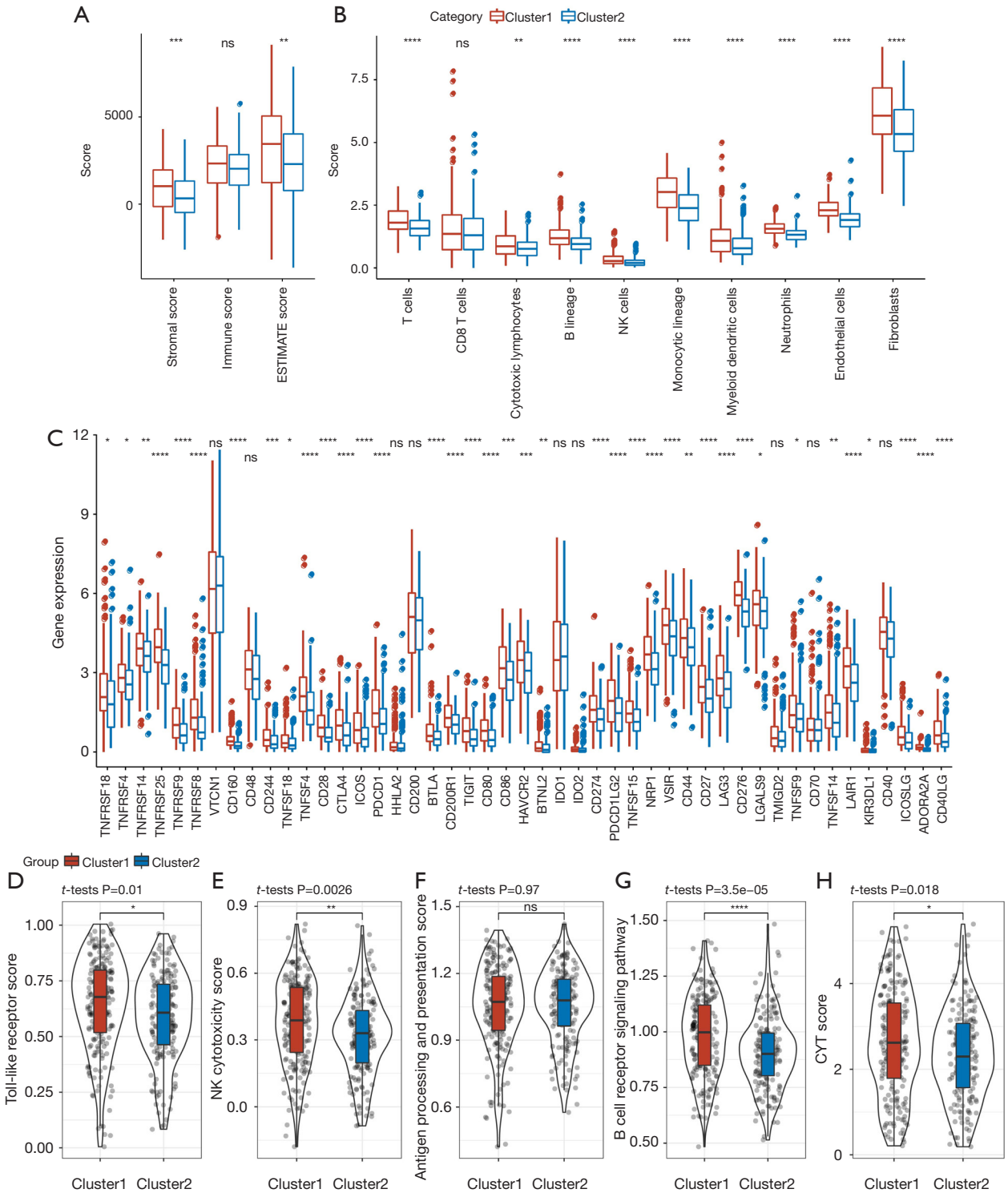

Figure 4 Analysis of the tumor immune microenvironment. (A) The differences in stromal score, immune score, and ESTIMATE score between the 2 clusters. (B) The differences in the scores of 10 kinds of immune cells between the 2 clusters. (C) The expression levels of immune checkpoint genes between the 2 clusters. (D-G) Score differences of the Toll-like receptor signaling pathway, natural killer cell-mediated cytotoxicity, antigen processing and presentation, and the B cell receptor signaling pathway between the 2 clusters. (H) CYT score differences between the 2 clusters. *P<0.05; **P<0.01; ***P<0.001; ****P<0.0001. ns, no significance; ESTIMATE, Estimation of Stromal and Immune cells in Malignant Tumors using Expression data; NK, natural killer; CYT, cytolytic activity.

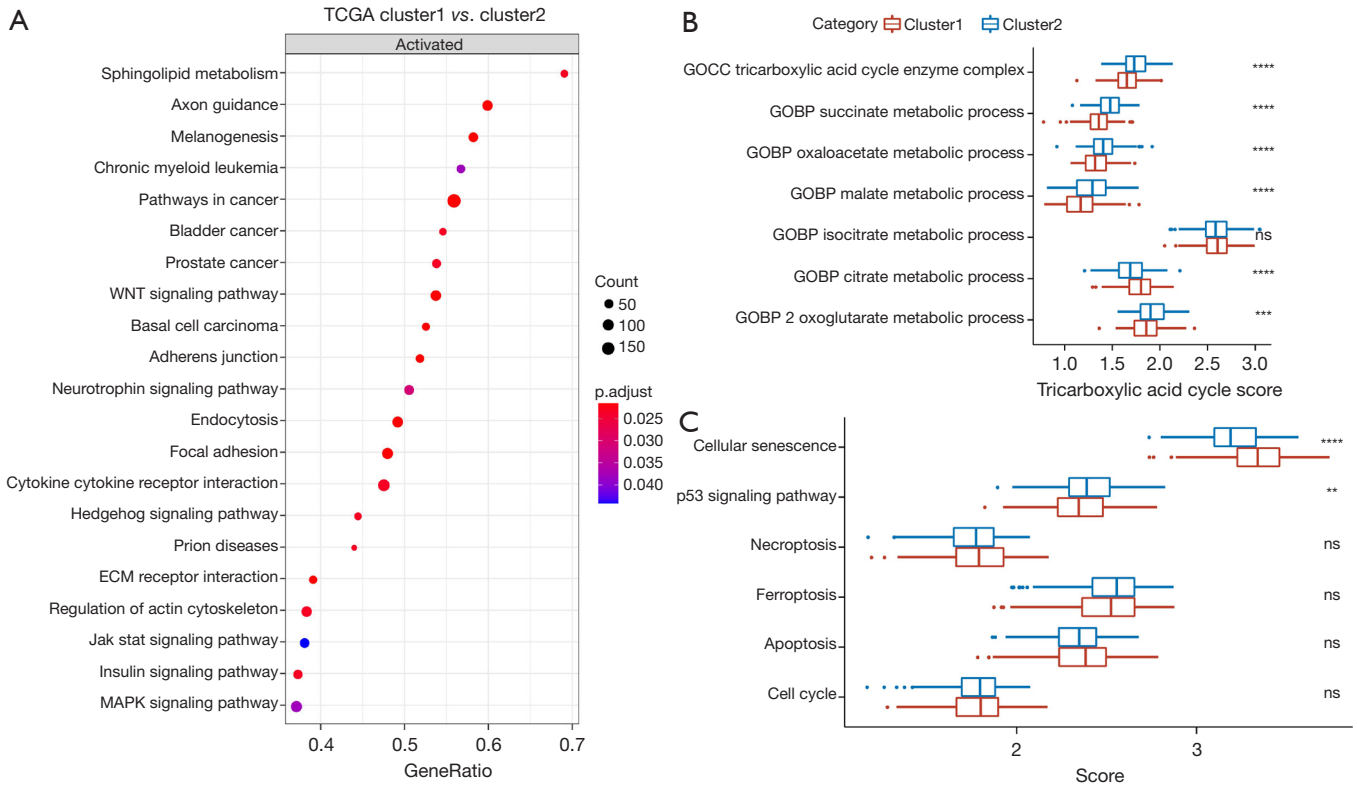

Figure 5 Functional enrichment analysis. (A) GSEA showed that many cancer-related pathways were activated in C1. (B) TCA-related pathway scores presented differences between the 2 clusters. (C) Score differences of pathways involved in cell growth and death between the 2 clusters. **P<0.01; ***P<0.001; ****P<0.0001. TCGA, The Cancer Genome Atlas; ns, no significance; GSEA, gene set enrichment analysis; TCA, tricarboxylic acid; ECM, extracellular matrix.

epithelial-mesenchymal transition, the mitogen activated protein kinase (MAPK) pathway, and other signaling pathways, and can also regulate autophagy and promote angiogenesis, thereby affecting the proliferation and metastasis of tumor cells (21,22). Kordestani *et al.* (23) pointed out that copper complex 3,5 dibromine salicylaldehyde imide combined with copper nitrate, synthesized from raw materials such as copper nitrate, ethylenediamine, 3, 5-dibromine salicylaldehyde, and triethylamine, can inhibit the proliferation of human A2780 ovarian cancer cells. Luo *et al.* (24) prepared a simple and feasible biotinylated copper containing complex, namely biotin cuprous chloride complex (Bio-cucL), in which the biotin part could target biotin receptor-positive tumor cells and specifically kill tumor cells. Copper transporting ATPase α (*ATP7A*) and copper transporting ATPase β (*ATP7B*) are copper transporters which mediate the transport and excretion of copper ions. A study has found that the high expression of *ATP7A* and *ATP7B* is associated with poor prognosis and resistance to platinum-based drugs in patients with ovarian cancer, non-small cell lung cancer, and colorectal cancer (25). Previous research confirmed the vital role of copper ions in cancer. Also, there are several cuproptosis-related gene signatures, analyzed by bioinformatics, which could predict the prognosis of clear cell renal cell carcinoma (13), HCC (12), and soft tissue sarcoma (26). In our study, we successfully established a cuproptosis-related classification system and an 8 cuproptosis-related gene signature.

AMER1, *ATP2A3*, *HIPK2*, *RRP12*, *VANGL1*, *JAG2*, *GALNT6*, and *CD79A* were used to construct the 8 cuproptosis-related gene signature. A previous structural analysis indicated that *AMER1* binds with *APC* and was used as an inhibitor of the Wnt/β-catenin signaling pathway (27).

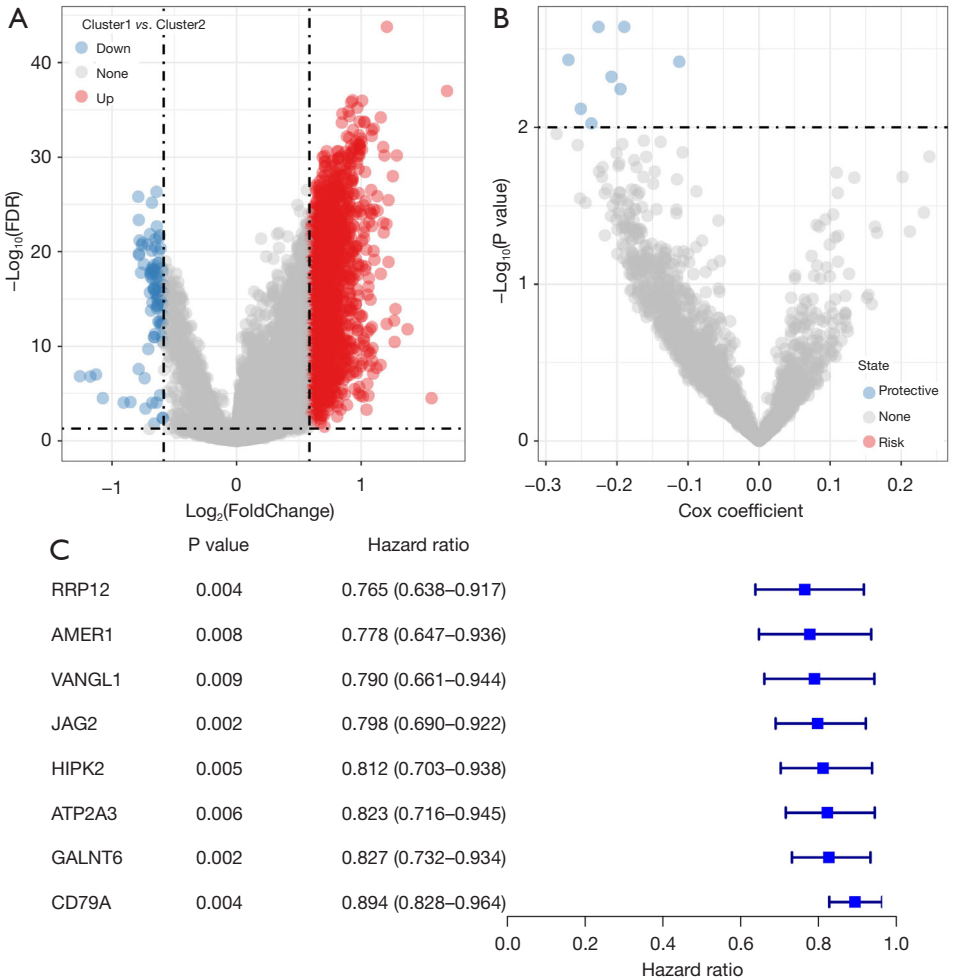

Figure 6 Identification of hub genes associated with cuproptosis. (A) Volcano plot of differentially expressed genes between the 2 clusters. (B) Volcano plot of 8 potential candidate genes. (C) Forest plot of 8 genes based on univariate Cox regression. FDR, false discovery rate.

Griffin *et al.* reported that *ATP2A3* expression was decreased in Jurkat cells, reducing the transport of calcium from the cytoplasm into the endoplasmic reticulum (28). *HIPK2* inhibits tumor growth by suppressing angiogenesis (29). *RRP12* is more highly expressed and used as a biomarker for the prognosis of colorectal cancer (30). The cancer-promoting effects of *VANGL1* and *JAG2* on cell proliferation and invasion have been found in various tumors (31-34). *GALNT6* exhibits oncogenic functions in breast cancer and ovarian cancer (35,36).

We are required to note the limitations of our work. In the future, we plan to place a greater emphasis on research that is both fundamentally experimental and functionally in-depth. Other considerations were not taken into account on our end because the samples lacked essential clinical follow-up information, most notably diagnostic specifics., such as whether or not the patients had other health conditions, when differentiating the molecular sub-types.

Conclusions

This study systematically analyzed the landscape of molecular alterations and interactive genes of cuproptosis in ovarian cancer. The prognostic risk score based on the

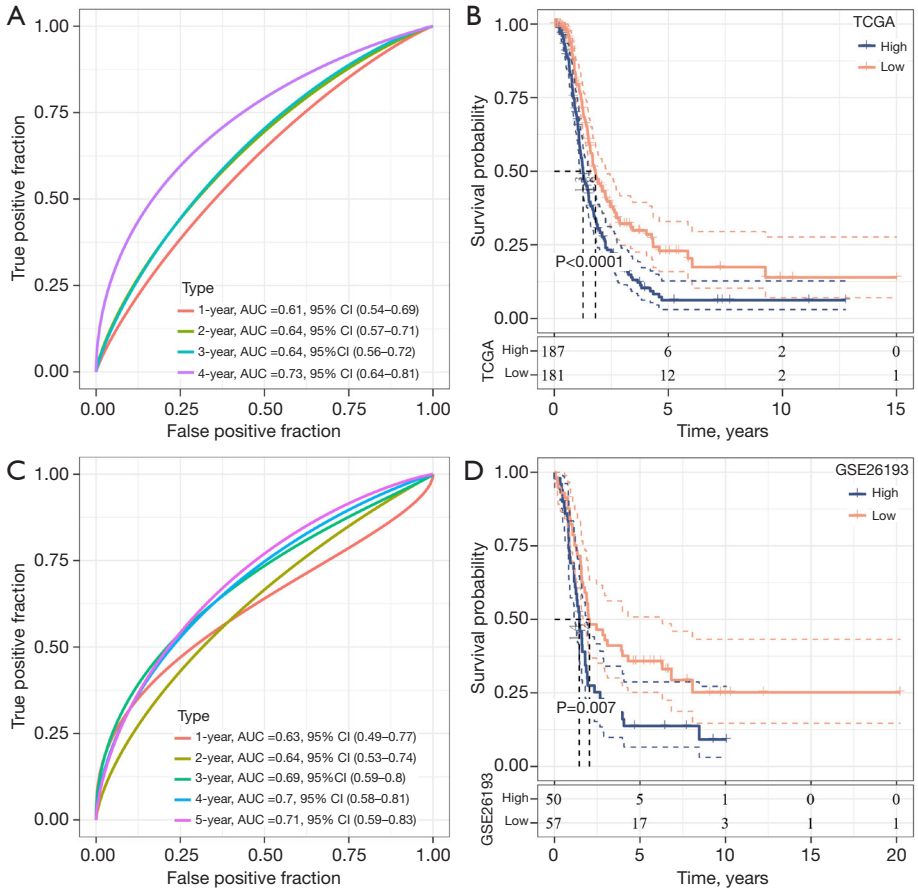

Figure 7 Validation of the risk score. (A) ROC curve of the risk score in TCGA-ovarian cancer dataset. (B) KM survival curve between the high group and low group in TCGA-ovarian cancer dataset. (C) ROC curve of the risk score in the GSE26193 dataset. (D) KM survival curve between the high group and low group in the GSE26193 dataset. AUC, area under the curve; CI, confidence interval; TCGA, The Cancer Genome Atlas; ROC, receiver operating characteristic; KM, Kaplan-Meier.

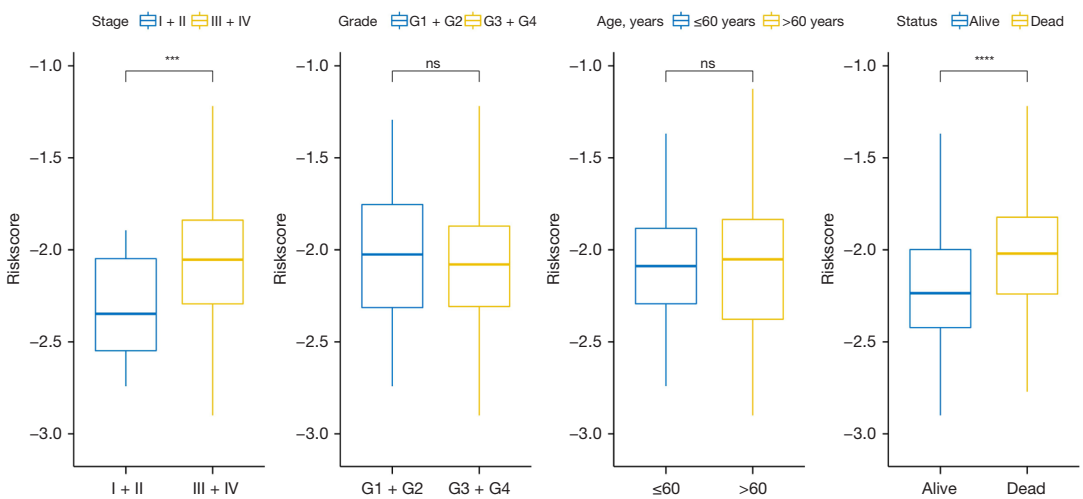

Figure 8 The distributions of clinical features, stage, grade, age, and status in the high group and low group. ***P<0.001; ****P<0.0001. ns, no significance.

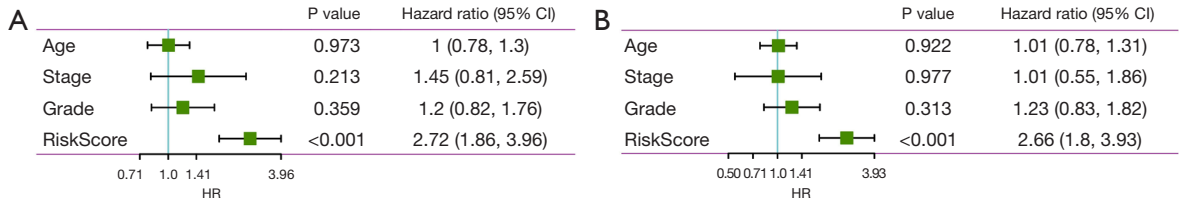

Figure 9 Independent prognostic ability of the risk score. (A) Univariate Cox survival analysis. (B) Multivariate Cox survival analysis. CI, confidence interval; HR, hazard ratio.

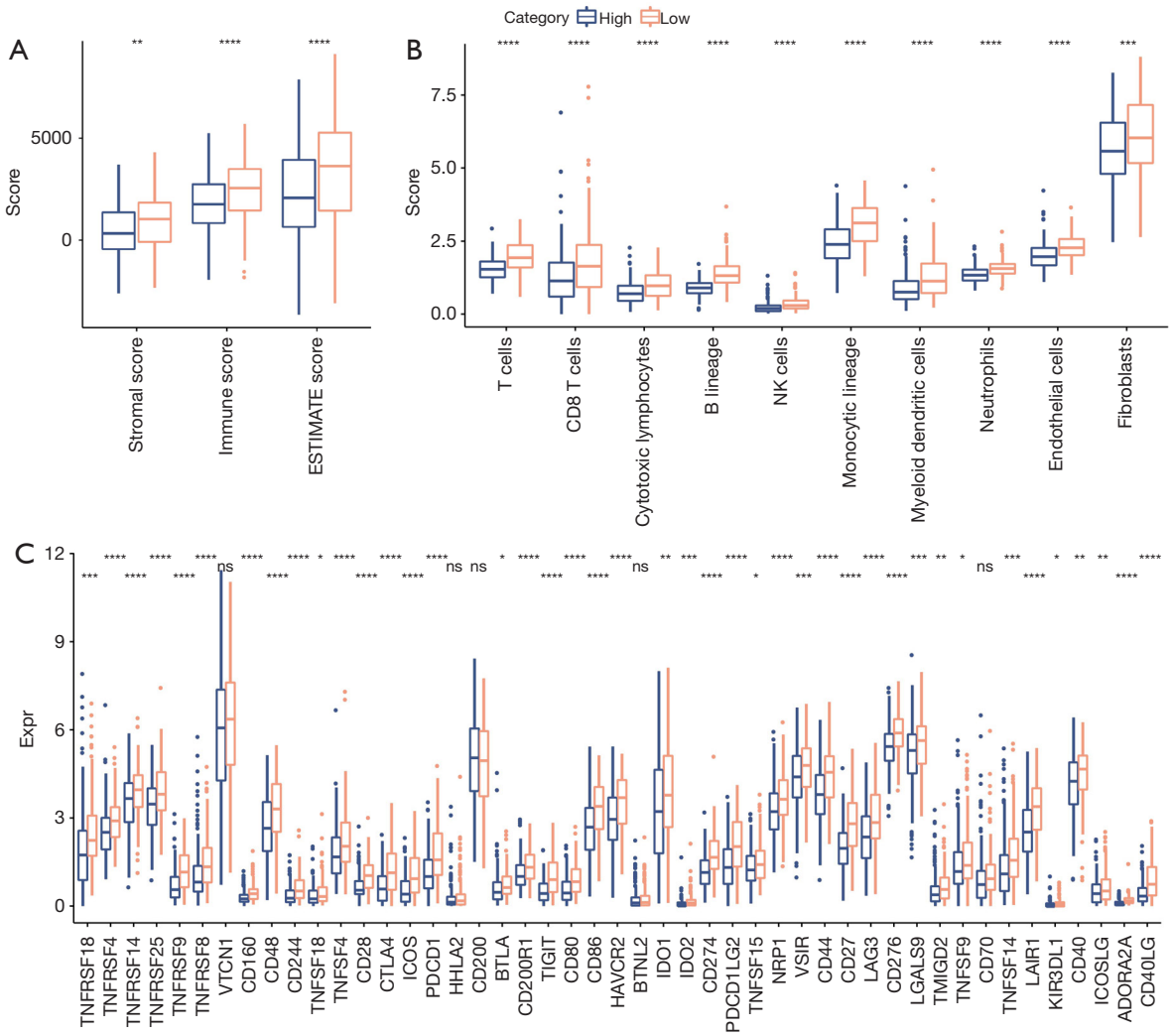

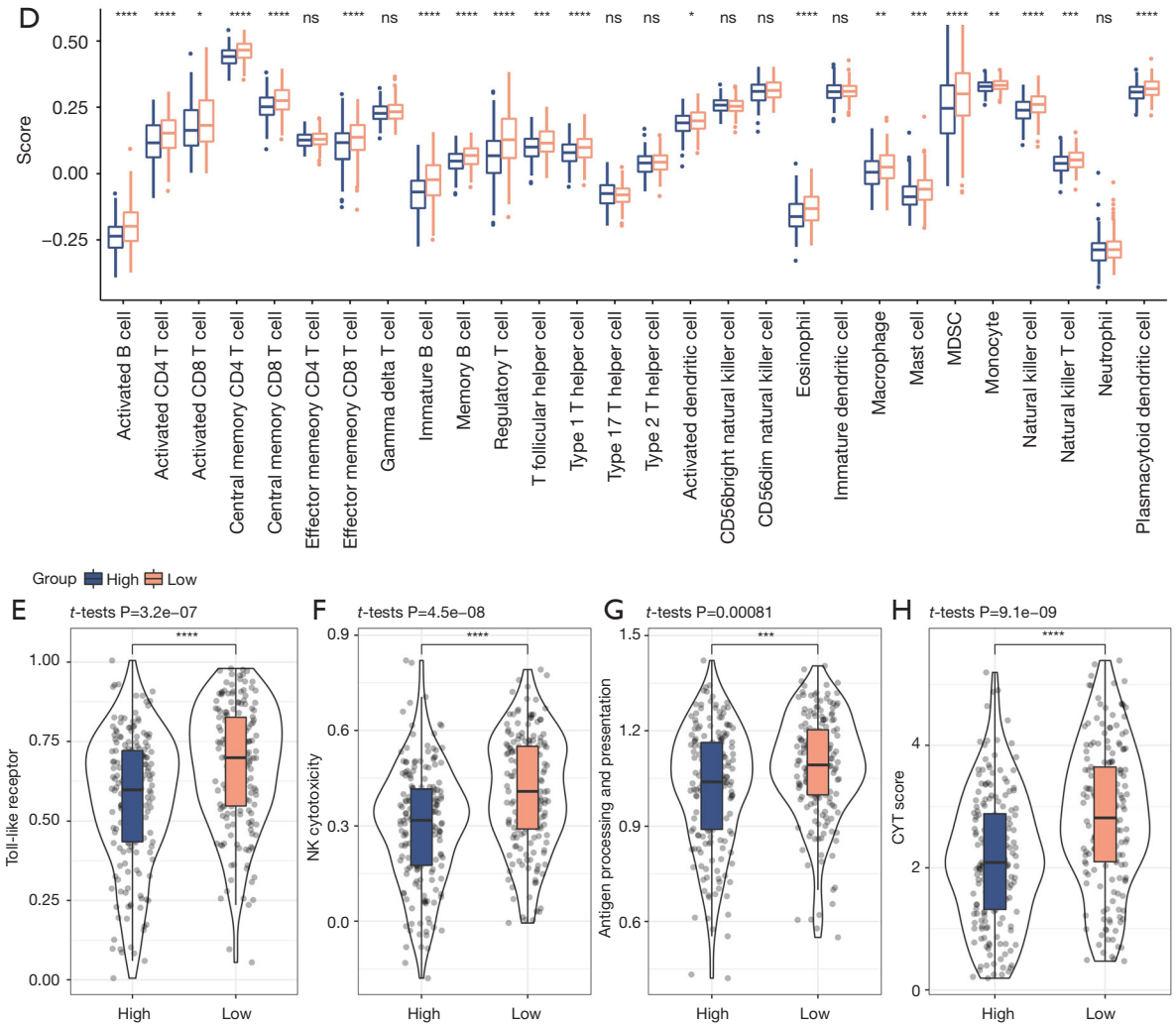

Figure 10 Analysis of the tumor immune microenvironment. (A) The differences in stromal score, immune score, and ESTIMATE score between the high group and low group. (B) The differences in scores of 10 kinds of immune cells between the high group and low group. (C) The expression levels of immune checkpoint genes between the high group and low group. (D) The differences in scores of 28 kinds of immune cells between the high group and low group. (E-G) Score differences of the Toll-like receptor signaling pathway, natural killer cell mediated cytotoxicity, and antigen processing and presentation between the high group and low group. (H) CYT score differences between the high group and low group. *P<0.05; **P<0.01; ***P<0.001; ****P<0.0001. ns, no significance; ESTIMATE, Estimation of Stromal and Immune cells in Malignant Tumors using Expression data; CYT, cytolytic activity; NK, natural killer.

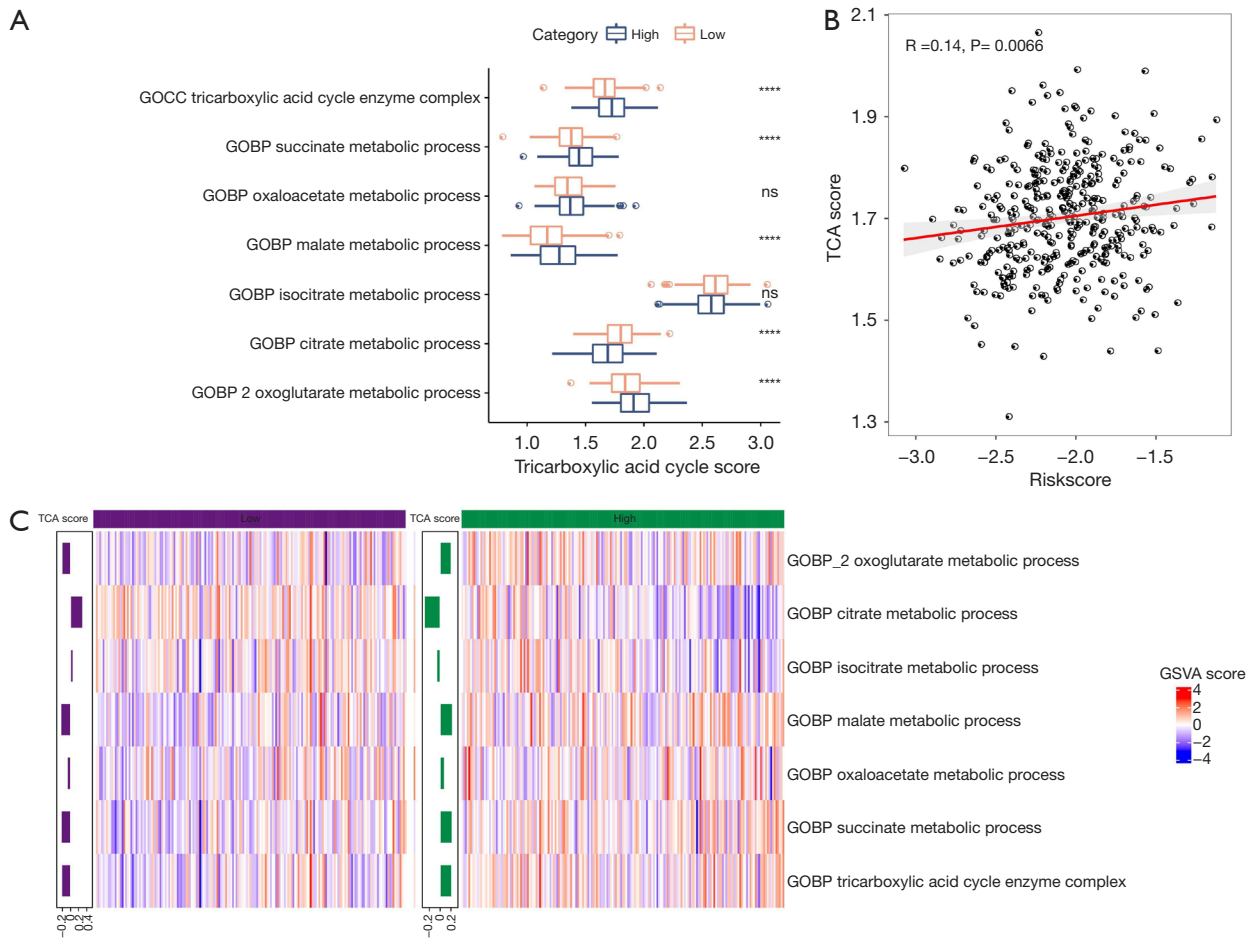

Figure 11 TCA pathway analysis of the risk score. (A) TCA-related pathway scores had significantly differences between the 2 groups. (B) Heatmap analysis indicated that the high group had higher TCA pathway scores. (C) TCA score was positively correlated with risk score. ****P<0.0001. ns, no significance; TCA, tricarboxylic acid; GSVA, gene set variation analysis.

expression signature of cuproptosis-related genes showed good performance for the prediction of the OS of ovarian cancer patients and was significantly associated with immune infiltration levels and TCA pathways. Our results will also provide new insights into the development of therapeutic strategies for the treatment and prognosis of ovarian cancer.

Acknowledgments

Funding: None.

Footnote

Reporting Checklist: The authors have completed the TRIPOD reporting checklist. Available at https://atm.amegroups.com/article/view/10.21037/atm-22-4546/rc

Conflicts of Interest: All authors have completed the ICMJE uniform disclosure form (available at https://atm.amegroups.com/article/view/10.21037/atm-22-4546/coif). The authors have no conflicts of interest to declare.

Ethical Statement: The authors are accountable for all aspects of the work, including ensuring that any questions related to the accuracy or integrity of any part of the work have been appropriately investigated and resolved. The study was conducted in accordance with the Declaration of Helsinki (as revised in 2013).

References

1. Sung H, Ferlay J, Siegel RL, et al. Global Cancer Statistics 2020: GLOBOCAN Estimates of Incidence and Mortality Worldwide for 36 Cancers in 185 Countries. CA Cancer J Clin 2021;71:209-49.
2. Chen W, Zheng R, Baade PD, et al. Cancer statistics in China, 2015. CA Cancer J Clin 2016;66:115-32.
3. Moss HA, Berchuck A, Neely ML, et al. Estimating Cost-effectiveness of a Multimodal Ovarian Cancer Screening Program in the United States: Secondary Analysis of the UK Collaborative Trial of Ovarian Cancer Screening (UKCTOCS). JAMA Oncol 2018;4:190-5.
4. Kajiyama H, Shibata K, Mizuno M, et al. Long-term survival of young women receiving fertility-sparing surgery for ovarian cancer in comparison with those undergoing radical surgery. Br J Cancer 2011;105:1288-94.
5. Arredondo M, Núñez MT. Iron and copper metabolism. Mol Aspects Med 2005;26:313-27.
6. Tsvetkov P, Coy S, Petrova B, et al. Copper induces cell death by targeting lipoylated TCA cycle proteins. Science 2022;375:1254-61.
7. Rostkowska-Nadolska B, Pośpiech L, Bochnia M. Content of trace elements in serum of patients with carcinoma of the larynx. Arch Immunol Ther Exp (Warsz) 1999;47:321-5.
8. Kuo HW, Chen SF, Wu CC, et al. Serum and tissue trace elements in patients with breast cancer in Taiwan. Biol Trace Elem Res 2002;89:1-11.
9. Garber K. Cancer's copper connections. Science 2015;349:129.
10. Ren X, Li Y, Zhou Y, et al. Overcoming the compensatory elevation of NRF2 renders hepatocellular carcinoma cells more vulnerable to disulfiram/copper-induced ferroptosis. Redox Biol 2021;46:102122.
11. Yang M, Wu X, Hu J, et al. COMMD10 inhibits HIF1α/CP loop to enhance ferroptosis and radiosensitivity by disrupting Cu-Fe balance in hepatocellular carcinoma. J Hepatol 2022;76:1138-50.
12. Zhang G, Sun J, Zhang X. A novel Cuproptosis-related LncRNA signature to predict prognosis in hepatocellular carcinoma. Sci Rep 2022;12:11325.
13. Bian Z, Fan R, Xie L. A Novel Cuproptosis-Related Prognostic Gene Signature and Validation of Differential Expression in Clear Cell Renal Cell Carcinoma. Genes (Basel) 2022;13:851.
14. Lei L, Tan L, Sui L. A novel cuproptosis-related gene signature for predicting prognosis in cervical cancer. Front Genet 2022;13:957744.
15. Wilkerson MD, Hayes DN. ConsensusClusterPlus: a class discovery tool with confidence assessments and item tracking. Bioinformatics 2010;26:1572-3.
16. Liu F, Qian J, Ma C. MPscore: A Novel Predictive and Prognostic Scoring for Progressive Meningioma. Cancers (Basel) 2021;13:1113.
17. Charoentong P, Finotello F, Angelova M, et al. Pan-cancer Immunogenomic Analyses Reveal Genotype-Immunophenotype Relationships and Predictors of Response to Checkpoint Blockade. Cell Rep 2017;18:248-62.
18. Yang P, Chen W, Xu H, et al. Correlation of CCL8 expression with immune cell infiltration of skin cutaneous melanoma: potential as a prognostic indicator and therapeutic pathway. Cancer Cell Int 2021;21:635.
19. Liu Y, He M, Wang D, et al. HisgAtlas 1.0: a human immunosuppression gene database. Database (Oxford) 2017;2017:bax094.
20. Shen W, Song Z, Xiao Z, et al. Sangerbox: A comprehensive, interaction-friendly clinical bioinformatics analysis platform. iMeta 2022;1:e36.
21. da Silva DA, De Luca A, Squitti R, et al. Copper in tumors and the use of copper-based compounds in cancer treatment. J Inorg Biochem 2022;226:111634.
22. Shanbhag VC, Gudekar N, Jasmer K, et al. Copper metabolism as a unique vulnerability in cancer. Biochim Biophys Acta Mol Cell Res 2021;1868:118893.
23. Kordestani N, Rudbari HA, Fernandes AR, et al. Antiproliferative Activities of Diimine-Based Mixed Ligand Copper(II) Complexes. ACS Comb Sci 2020;22:89-99.
24. Luo B, Chen L, Hong Z, et al. A simple and feasible atom-precise biotinylated Cu(i) complex for tumor-targeted chemodynamic therapy. Chem Commun (Camb) 2021;57:6046-9.
25. Li YQ, Yin JY, Liu ZQ, et al. Copper efflux transporters ATP7A and ATP7B: Novel biomarkers for platinum drug resistance and targets for therapy. IUBMB Life 2018;70:183-91.
26. Han J, Hu Y, Liu S, et al. A Newly Established Cuproptosis-Associated Long Non-Coding RNA

Signature for Predicting Prognosis and Indicating Immune Microenvironment Features in Soft Tissue Sarcoma. J Oncol 2022;2022:8489387.
27. Grohmann A, Tanneberger K, Alzner A, et al. AMER1 regulates the distribution of the tumor suppressor APC between microtubules and the plasma membrane. J Cell Sci 2007;120:3738-47.
28. Griffin JB, Rodriguez-Melendez R, Dode L, et al. Biotin supplementation decreases the expression of the SERCA3 gene (ATP2A3) in Jurkat cells, thus, triggering unfolded protein response. J Nutr Biochem 2006;17:272-81.
29. Chen P, Duan X, Li X, et al. HIPK2 suppresses tumor growth and progression of hepatocellular carcinoma through promoting the degradation of HIF-1α. Oncogene 2020;39:2863-76.
30. Hu M, Fu X, Si Z, et al. Identification of Differently Expressed Genes Associated With Prognosis and Growth in Colon Adenocarcinoma Based on Integrated Bioinformatics Analysis. Front Genet 2019;10:1245.
31. Sun EG, Lee KH, Ko YS, et al. KITENIN functions as a fine regulator of ErbB4 expression level in colorectal cancer via protection of ErbB4 from E3-ligase Nrdp1-mediated degradation. Mol Carcinog 2017;56:1068-81.
32. Hao CC, Xu CY, Zhao XY, et al. Up-regulation of VANGL1 by IGF2BPs and miR-29b-3p attenuates the detrimental effect of irradiation on lung adenocarcinoma. J Exp Clin Cancer Res 2020;39:256.
33. Li CY, Miao KL, Chen Y, et al. Jagged2 promotes cancer stem cell properties of triple negative breast cancer cells and paclitaxel resistance via regulating microRNA-200. Eur Rev Med Pharmacol Sci 2018;22:6008-14.
34. Yang F, Zhao WJ, Jia CL, et al. MicroRNA-876-3p functions as a tumor suppressor gene and correlates with cell metastasis in pancreatic adenocarcinoma via targeting JAG2. Am J Cancer Res 2018;8:636-49.
35. Sheta R, Bachvarova M, Macdonald E, et al. The polypeptide GALNT6 Displays Redundant Functions upon Suppression of its Closest Homolog GALNT3 in Mediating Aberrant O-Glycosylation, Associated with Ovarian Cancer Progression. Int J Mol Sci 2019;20:2264.
36. Park JH, Nishidate T, Kijima K, et al. Critical roles of mucin 1 glycosylation by transactivated polypeptide N-ace tylgalactosaminyltransferase 6 in mammary carcinogenesis. Cancer Res 2010;70:2759-69.

(English Language Editor: C. Betlazar-Maseh)

Cite this article as: Sun X, Xu P, Zhang F, Sun T, Jiang H, Lu X, Zhang M, Li P. The cuproptosis-related gene signature serves as a potential prognostic predictor for ovarian cancer using bioinformatics analysis. Ann Transl Med 2022;10(18):1021. doi: 10.21037/atm-22-4546

